Inorg. Chem. **2005**, *44*, 9489–9496

A Chloro-Bridged Dimanganese Complex and an Oxo-Bridged Dititanium Complex of a Ditopic Bis(pyrazol-1-yl)borate Ligand

Susanne Bieller, Michael Bolte, Hans-Wolfram Lerner, and Matthias Wagner*

Institut für Anorganische Chemie, J. W. Goethe-Universität Frankfurt, Marie-Curie-Strasse 11, D-60439 Frankfurt (Main), Germany

Received September 30, 2005

The synthesis and crystal structure analysis of the ditopic *p*-phenylene-bridged bis(pyrazol-1-yl)borate [[*p*-C_6H_4-($Bpz_2tBu)_2$]Li_2] (LLi_2; pz = pyrazol-1-yl) is described. A salt metathesis reaction between LLi_2 and $MnCl_2$ in THF leads to the dinuclear complex [L[Mn(THF)]$_2$(μ-Cl)$_2$] featuring a central diamond Mn^{II}–(μ-Cl)$_2$–Mn^{II} core (X-ray crystal structure analysis). Treatment of LLi_2 with 2 equiv of [Ti(NMe_2)$_3$Cl] gives the dinuclear titanium compound [L[Ti(NMe_2)$_3$]$_2$]. Upon reaction of LLi_2 with [Ti(NMe_2)$_2$Cl$_2$] and water, the μ-oxo-bridged dititanium species [L[Ti(NMe_2)Cl]$_2$(μ-O)] is obtained in excellent yield (X-ray crystal structure analysis).

Introduction

Because of their versatility and a modular synthesis approach that allows extensive modifications of the molecular framework, bis- and tris(pyrazol-1-yl)borates ("scorpionates") have found widespread use in organometallic and coordination chemistry, with applications ranging from modeling active sites of metalloenzymes through catalysis to materials sciences.[1,2] Even though dinuclear complexes are of particular interest in many of these areas,[3−6] only a surprisingly small number of ditopic scorpionate ligands is known to date. In 1988, Niedenzu published the discorpionate **A**, which is based on diborane(4) (Figure 1).[7] Metal complexes (i.e., K, Mo, Pd, La, Eu, Gd, and Tb) of derivatives of **A** were subsequently prepared by Niedenzu and Ward.[8−10] A few years ago, our group developed a synthetic procedure for the redox-active, ferrocene-based ligand **B** (Figure 1, R = pz, Me; pz = pyrazol-1-yl),[11,12] and described its coordination chemistry (K, Zr, Mo, and Tl).[13] More recently, we published the *m*- and *p*-phenylene-bridged ditopic bis(pyrazol-1-yl)borates **C** and **D** (Figure 1).[14] Neutral bis(pyrazol-1-yl)methane analogues of **B**, **C**, and **D** were prepared by Reger et al.[15−17]

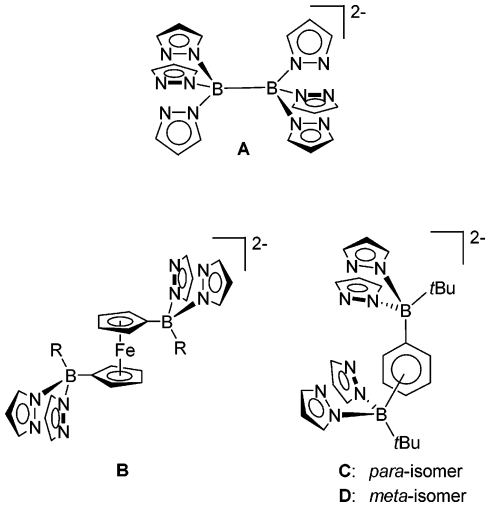

Figure 1. Ditopic scorpionate ligands **A**, **B** (R = pz, Me), **C**, and **D**.

* To whom correspondence should be addressed. E-mail: Matthias.Wagner@chemie.uni-frankfurt.de.

(1) Trofimenko, S. *Chem. Rev.* **1993**, *93*, 943−980.
(2) Trofimenko, S. *Scorpionates—The Coordination Chemistry of Polypyrazolylborate Ligands*; Imperial College Press: London, 1999.
(3) Adams, R. D., Cotton, F. A., Eds. *Catalysis by Di- and Polynuclear Metal Cluster Complexes*; Wiley: New York, 1998.
(4) Martell, A. E.; Perutka, J.; Kong, D. *Coord. Chem. Rev.* **2001**, *216−217*, 55−63.
(5) Mathonière, C.; Sutter, J.-P.; Yakhmi, J. V. In *Magnetism: Molecules to Materials IV*; Miller, J. S., Drillon, M., Eds.; Wiley-VCH: Weinheim, Germany, 2002.
(6) Gavrilova, A. L.; Bosnich, B. *Chem. Rev.* **2004**, *104*, 349−383.
(7) Brock, C. P.; Das, M. K.; Minton, R. P.; Niedenzu, K. *J. Am. Chem. Soc.* **1988**, *110*, 817−822.
(8) Harden, N. C.; Jeffery, J. C.; McCleverty, J. A.; Rees, L. H.; Ward, M. D. *New J. Chem.* **1998**, *22*, 661−663.
(9) Armaroli, N.; Accorsi, G.; Barigelletti, F.; Couchman, S. M.; Fleming, J. S.; Harden, N. C.; Jeffery, J. C.; Mann, K. L. V.; McCleverty, J. A.; Rees, L. H.; Starling, S. R.; Ward, M. D. *Inorg. Chem.* **1999**, *38*, 5769−5776.
(10) Farley, R. D.; Hoefer, P.; Maher, J. P.; McCleverty, J. A.; Murphy, D. M.; Rowlands, C. C.; Ung, V. A.; Ward, M. D. *Magn. Reson. Chem.* **2002**, *40*, 683−686.
(11) Jäkle, F.; Polborn, K.; Wagner, M. *Chem. Ber.* **1996**, *129*, 603−606.
(12) Haghiri Ilkhechi, A.; Bolte, M.; Lerner, H.-W.; Wagner, M. *J. Organomet. Chem.* **2005**, *690*, 1971−1977.
(13) Fabrizi de Biani, F.; Jäkle, F.; Spiegler, M.; Wagner, M.; Zanello, P. *Inorg. Chem.* **1997**, *36*, 2103−2111.

10.1021/ic051689h CCC: $30.25
Published on Web 11/17/2005

For a systematic investigation of the coordination behavior of **C** and **D**, we started with complexes of **D** with the soft monovalent metal ions Tl^I, Cu^I, and Ag^I.[18] The thallium ion was chosen because Tl^I scorpionates are known to be useful ligand-transfer reagents for the synthesis of the corresponding transition-metal complexes.[19] Cu^I and Ag^I scorpionates are of interest because they may serve as efficient catalysts for the activation of unfunctionalized hydrocarbons via metal-mediated carbene insertion.[20,21]

We now extend our study to middle and early first-row transition metals, as they play an important role in many industrial catalysts and metal-containing enzymes. The bacterial enzyme manganese catalase, for example, which is involved in the disproportionation of hydrogen peroxide to dioxygen and water and thus in the protection of the cells from hydroxyl radicals, possesses an active site containing two manganese centers (Mn^{II}/Mn^{II}; Mn^{III}/Mn^{III}) bridged by small molecules (H_2O, OH^-, $RCOO^-$).[22,23] With respect to industrial catalysis, titanium complexes are of ample interest in olefin polymerization reactions.[24−27] In the context of this paper, two recent developments are particularly important: (i) Titanium poly(pyrazol-1-yl)borates have been employed in the homopolymerization of ethylene and styrene as well as in their copolymerization with 1-hexene.[28−33] (ii) Dinuclear Ti^{IV} and Zr^{IV} complexes and the role of cooperative effects on the performance of these catalysts have been outlined in several papers[34−45] and patents.[46−51]

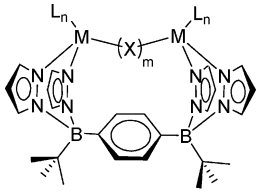

E

Figure 2. Bridged coordination mode of dinuclear complexes **E**.

The purpose of this paper is to describe dinuclear Mn^{II} and Ti^{IV} complexes of the *p*-phenylene-bridged bis(pyrazol-1-yl)borate ligand **C**. Special emphasis is put on the question of whether the ligand is well enough designed to allow simultaneous binding of both metal centers to the same substrate molecule (cf. **E**, Figure 2).

Results and Discussion

Syntheses and Spectroscopy. Both for the purification of poly(pyrazol-1-yl)borate ligands and for the preparation of the corresponding transition-metal complexes, thallium scorpionates are particularly well-suited. The K^+ ion is similar to Tl^+ in size and charge, but is much less toxic. Whenever possible, potassium scorpionates are thus preferred for ligand characterization and complex synthesis. Accordingly, ligand **C** was first prepared in the form of its potassium salt (LK_2; in molecular formulas, the free ligand [*p*-C_6H_4-$(Bpz_2tBu)_2]^{2-}$ will be abbreviated as L^{2-}).[14] Because first efforts to transform LK_2 into transition-metal complexes did not give fully satisfactory results, we decided to also prepare the lithium salt LLi_2. The synthesis started from *p*-C_6H_4-$[B(NMe_2)tBu]_2$ (**1**),[14] 2 equiv of pyrazole, and 2 equiv of lithium pyrazolide, and was performed in a procedure similar to that previously reported[14] for LK_2 (cf. **2**, Scheme 1). X-ray quality crystals of **2** formed upon layering its THF solution with toluene at room temperature. The ^{11}B NMR spectrum of **2** reveals one signal at 3.0 ppm, which indicates the presence of two magnetically equivalent tetracoordinated

(14) Bieller, S.; Zhang, F.; Bolte, M.; Bats, J. W.; Lerner, H.-W.; Wagner, M. *Organometallics* **2004**, *23*, 2107−2113.
(15) Reger, D. L.; Brown, K. J.; Gardinier, J. R.; Smith, M. D. *Organometallics* **2003**, *22*, 4973−4983.
(16) Reger, D. L.; Brown, K. J.; Gardinier, J. R.; Smith, M. D. *J. Organomet. Chem.* **2005**, *690*, 1889−1900.
(17) Reger, D. L.; Watson, R. P.; Smith, M. D.; Pellechia, P. J. *Organometallics* **2005**, *24*, 1544−1555.
(18) Zhang, F.; Bolte, M.; Lerner, H.-W.; Wagner, M. *Organometallics* **2004**, *23*, 5075−5080.
(19) Janiak, C. *Coord. Chem. Rev.* **1997**, *163*, 107−216.
(20) Rasika Dias, H. V.; Browning, R. G.; Richey, S. A.; Lovely, C. J. *Organometallics* **2004**, *23*, 1200−1202.
(21) Urbano, J.; Belderraín, T. R.; Nicasio, M. C.; Trofimenko, S.; Díaz-Requejo, M. M.; Pérez, P. J. *Organometallics* **2005**, *24*, 1528−1532.
(22) Dismukes, G. C. *Chem. Rev.* **1996**, *96*, 2909−2926.
(23) Barynin, V. V.; Hempstead, P. D.; Vagin, A. A.; Antonyuk, S. V.; Melik-Adamyan, W. R.; Lamzin, V. S.; Harrison, P. M.; Artymiuk, P. J. *J. Inorg. Biochem.* **1997**, *67*, 196.
(24) Boor, J., Jr. *Ziegler−Natta Catalysts and Polymerizations*; Academic Press: New York, 1979.
(25) Albizzati, E.; Galimberti, M. *Catal. Today* **1998**, *41*, 159−168.
(26) Razavi, A. *Hydrocarbon Eng.* **2003**, *8*, 27−30.
(27) Odian, G. *Principles of Polymerization*; Wiley: Hoboken, NJ, 2004.
(28) Nakazawa, H.; Ikai, S.; Imaoka, K.; Kai, Y.; Yano, T. *J. Mol. Catal. A: Chem.* **1998**, *132*, 33−41.
(29) Gil, M. P.; dos Santos, J. H. Z.; Casagrande, O. L., Jr. *Macromol. Chem. Phys.* **2001**, *202*, 319−324.
(30) Murtuza, S.; Casagrande, O. L., Jr.; Jordan, R. F. *Polym. Mater. Sci. Eng.* **2001**, *84*, 109−110.
(31) Murtuza, S.; Casagrande, O. L., Jr.; Jordan, R. F. *Organometallics* **2002**, *21*, 1882−1890.
(32) Gil, M. P.; Casagrande, O. L., Jr. *J. Organomet. Chem.* **2004**, *689*, 286−292.
(33) Gil, M. P.; dos Santos, J. H. Z.; Casagrande, O. L., Jr. *J. Mol. Catal. A: Chem.* **2004**, *209*, 163−169.
(34) Jüngling, S.; Mülhaupt, R.; Plenio, H. *J. Organomet. Chem.* **1993**, *460*, 191−195.
(35) Soga, K.; Ban, H. T.; Uozumi, T. *J. Mol. Catal. A: Chem.* **1998**, *128*, 273−278.
(36) Spaleck, W.; Kuber, F.; Bachmann, B.; Fritze, C.; Winter, A. *J. Mol. Catal. A: Chem.* **1998**, *128*, 279−287.
(37) Kang, K. K.; Hong, S.-P.; Jeong, Y.-T.; Shiono, T.; Ikeda, T. *J. Polym. Sci., Part A: Polym. Chem.* **1999**, *37*, 3756−3762.
(38) Noh, S. K.; Kim, J.; Jung, J.; Ra, C. S.; Lee, D.-H.; Lee, H. B.; Lee, S. W.; Huh, W. S. *J. Organomet. Chem.* **1999**, *580*, 90−97.
(39) Jung, J.; Noh, S. K.; Lee, D.-H.; Park, S. K.; Kim, H. *J. Organomet. Chem.* **2000**, *595*, 147−152.
(40) Xu, S.; Dai, X.; Wu, T.; Wang, B.; Zhou, X.; Weng, L. *J. Organomet. Chem.* **2002**, *645*, 212−217.
(41) Noh, S. K.; Kim, S.; Yang, Y.; Lyoo, W. S.; Lee, D.-H. *Eur. Polym. J.* **2004**, *40*, 227−235.
(42) Noh, S. K.; Lee, J.; Lee, D.-H. *J. Organomet. Chem.* **2003**, *667*, 53−60.
(43) Sierra, J. C.; Hüerländer, D.; Hill, M.; Kehr, G.; Erker, G.; Fröhlich, R. *Chem.−Eur. J.* **2003**, *9*, 3618−3622.
(44) Stojcevic, G.; Kim, H.; Taylor, N. J.; Marder, T. B.; Collins, S. *Angew. Chem., Int. Ed.* **2004**, *43*, 5523−5526.
(45) Deppner, M.; Burger, R.; Weiser, M.; Alt, H. G. *J. Organomet. Chem.* **2005**, *690*, 2861−2871.
(46) Ting, C.; Hua, S.-S.; Tsai, J.-C.; Wang, B.-P. EP 0985676, 2000.
(47) Tsai, J. C.; Liu, K.-K.; Chan, S.-H.; Wang, S.-J.; Young, M.-J.; Ting, C.; Hua, S.-S. EP 0985677, 2000.
(48) Devore, D. D.; Feng, S. S.; Frazier, K. A.; Graf, D. D.; Green, D. P. WO 58912, 2001.
(49) Graf, D. D.; Klosin, J.; Nickias, P. N.; Patton, J. T. U.S. 6235917, 2001.
(50) Do, Y.-K.; Cho, H.-S.; Yoon, S.-W.; Choi, K.-H.; Yoon, B.-S.; Kim, S.-K.; Han, Y.-G.; Park, S.-J.; Lee, J.-S. WO 2004/076502, 2004.
(51) Kim, E.-I.; Choi, S. D. U.S. 2004/0054207, 2004.

Scheme 1. Syntheses of the Ditopic Bis(pyrazol-1-yl)borate Ligand **2** and the Manganese Complex **3a**[a]

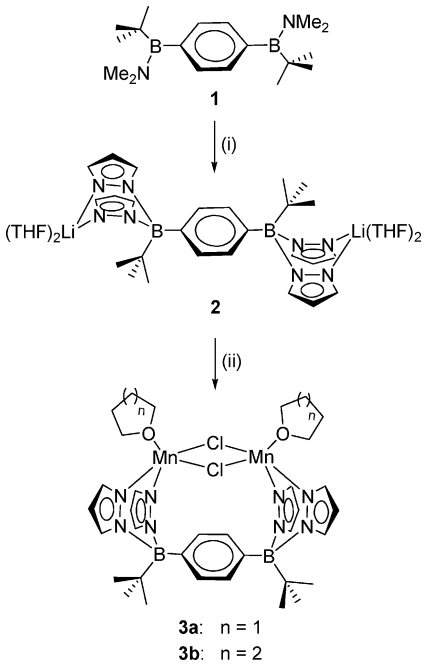

[a] (i) +2 equiv of Lipz/2 equiv of Hpz, toluene/THF, reflux. (ii) +$MnCl_2$, THF, rt.

boron centers.[52] Resonances at $\delta(^1H) = 7.33$ and $\delta(^{13}C) = 135.0$ are assigned to the *p*-phenylene bridge; signals at $\delta(^1H) = 0.66$ and $\delta(^{13}C) = 30.5$ originate from the *tert*-butyl groups. The pyrazolyl substituents give rise to three doublets of doublets at $\delta(^1H) = 5.93$, 7.05, and 7.42 ($\delta(^{13}C) = 102.1$, 137.7, and 137.9).

3a ($[L[Mn(THF)]_2(\mu\text{-}Cl)_2]$, Scheme 1) was synthesized via the reaction of **2** with 2 equiv of $MnCl_2$ in THF. Crystals suitable for an X-ray structure analysis were grown by slow diffusion of hexane into a THF solution of the crude product. Recrystallization of **3a** from tetrahydropyrane/hexane gave colorless blocks of **3b** (Scheme 1). In the NMR spectra of **3a** and **3b**, no signals could be detected because of the paramagnetic nature of these species. SQUID measurements on **3a** reveal two high-spin Mn^{II} centers that are weakly antiferromagnetically coupled via the chloro bridges.

We had to recognize on several occasions that ligand **D** is of limited stability in the presence of strongly Lewis acidic group 4 metal chlorides, which tend to induce B−N bond cleavage. In our efforts to prepare Ti^{IV} complexes of **C**, we thus decided to employ the less Lewis acidic dimethylamido derivatives $[Ti(NMe_2)_3Cl]$[53] and $[Ti(NMe_2)_2Cl_2]$.[53] Treatment of $[Ti(NMe_2)_3Cl]$ with **2** gave compound **4** ($[L[Ti(NMe_2)_3]_2]$, Scheme 2) in decent yield. X-ray quality crystals of **4** formed from its methylene chloride solution at −30 °C. The chemical-shift values (^{11}B, ^1H, ^{13}C) of complex **4** are very similar to those of **2** apart from the presence of additional signals that can be assigned to the dimethylamino groups ($\delta(^1H) = 3.06$, 36H; $\delta(^{13}C) = 47.8$).

Scheme 2. Syntheses of the Titanium Complexes **4** and **5**[a]

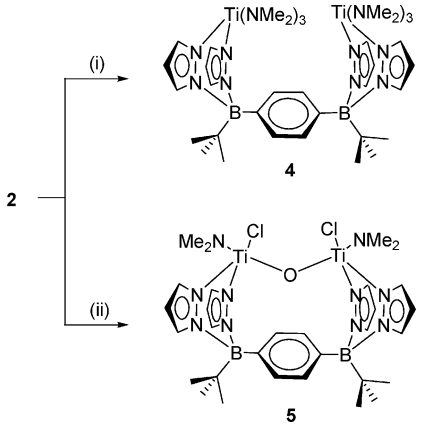

[a] (i) +2 equiv of $[Ti(NMe_2)_3Cl]$, toluene, −78 °C to rt. (ii) +2 equiv of $[Ti(NMe_2)_2Cl_2]\cdot 0.5H_2O$, THF, −78 °C to rt.

Attempts to create a Ti−O−Ti bridged species of type **E** (Figure 2) via purposeful hydrolysis[54] of **4** with 1 equiv of water failed. We hence prepared compound $[L[Ti(NMe_2)Cl]_2(\mu\text{-}O)]$ by conversion of **2** with a mixture of 2 equiv of $[Ti(NMe_2)_2Cl_2]$ and 1 equiv of H_2O (Scheme 2). X-ray quality crystals of **5** were grown from toluene/hexane. In C_6D_6, the two boron atoms of complex **5** give rise to one signal at 2.9 ppm, and are thus magnetically equivalent. In the ^1H NMR spectrum (C_6D_6), we observe one sharp singlet at 3.36 ppm, integrating for 12 H, which is assigned to two symmetry-related dimethylamido groups. The protons of the four pyrazolyl rings give rise to two sets of signals with equal intensity ($\delta(^1H) = 5.95$, 7.92, 8.26, and 6.01, 7.44, 7.85), whereas the C_6H_4 protons show a coupling pattern of two doublets (6.63 ppm, 6.84 ppm). Even at elevated temperatures (80 °C, C_6D_6), there is no coalescence of corresponding signals in the ^1H NMR spectrum. In contrast, the ^1H NMR spectrum of **4** shows only one signal for the phenylene bridge and one set of resonances for the four pyrazolyl moieties already at room temperature. The spectroscopic features of **5** may be explained by the presence of a C_2 axis (perpendicular to the *p*-phenylene plane) as the sole symmetry element. This interpretation is supported by the ^{13}C NMR spectrum of **5**, as it also shows two sets of signals for the phenylene and pyrazolyl carbon atoms, whereas both the *tert*-butyl substituents and the dimethylamido groups give rise to only one signal.

Crystal Structure Determinations. Crystal data and details of the structure determinations are summarized in Table 1. Selected bond lengths, atom···atom distances, bond angles, and torsion angles are listed in the figure captions. Lithium complex **2** crystallizes from THF/toluene in the orthorhombic space group *Pbca* (Figure 3), and consists of discrete dinuclear units arranged in approximate C_2 symmetry (axis orthogonal to the central phenylene ring). Only five other examples of structurally characterized lithium scorpionates are listed in the current version of the Cambridge Structural Database,[55] and just two of them show a tetrahedral

(52) Nöth, H.; Wrackmeyer, B. *Nuclear Magnetic Resonance Spectroscopy of Boron Compounds*; NMR Basic Principles and Progress; Diehl, P., Fluck, E., Kosfeld, R., Eds.; Springer-Verlag: New York, 1978; Vol. 14.
(53) Benzing, E.; Kornicker, W. *Chem. Ber.* **1961**, *94*, 2263−2267.
(54) Kuhn, N.; Maichle-Mössmer, C.; Weyers, G. *Z. Anorg. Allg. Chem.* **1999**, *625*, 851−856.
(55) Allen, F. H. *Acta Crystallogr., Sect. B* **2002**, *58*, 380−388.

Table 1. Crystal Data and Structure Refinement Details for **2**, **3b**·THP, **4**·$2CH_2Cl_2$, and **5**·C_7H_8·C_6H_{14}

	2	**3b**·THP	**4**·$2CH_2Cl_2$	**5**·C_7H_8·C_6H_{14}
formula	$C_{42}H_{66}B_2Li_2N_8O_4$	$C_{36}H_{54}B_2Cl_2Mn_2N_8O_2$ ·$C_5H_{10}O$	$C_{38}H_{70}B_2N_{14}Ti_2$ ·$2CH_2Cl_2$	$C_{30}H_{46}B_2Cl_2N_{10}OTi_2$ ·C_7H_8·C_6H_{14}
fw	782.53	919.40	1010.35	929.39
color, shape	colorless, block	colorless, block	dark red, block	orange, plate
T (K)	173(2)	173(2)	173(2)	173(2)
radiation, λ (Å)	Mo Kα, 0.71073	Mo Kα, 0.71073	Mo Kα, 0.71073	Mo Kα, 0.71073
cryst syst	orthorhombic	monoclinic	monoclinic	monoclinic
space group	*Pbca*	*P*2/*c*	$P2_1/c$	*C*2/*c*
a (Å)	19.617(2)	12.9081(6)	8.9956(15)	10.0340(18)
b (Å)	16.5862(16)	13.5164(8)	17.041(2)	31.270(4)
c (Å)	27.867(3)	13.9807(7)	19.519(4)	17.092(3)
α (deg)	90	90	90	90
β (deg)	90	106.833(4)	93.376(15)	91.360(15)
γ (deg)	90	90	90	90
V (Å^3)	9067.1(16)	2334.7(2)	2987.0(9)	5361.3(15)
Z	8	2	2	4
D_{calcd} (g cm^{-3})	1.146	1.308	1.123	1.151
F(000)	3376	968	1068	1968
μ (mm^{-1})	0.073	0.700	0.484	0.437
cryst size (mm)	0.33 × 0.28 × 0.14	0.24 × 0.18 × 0.11	0.24 × 0.21 × 0.20	0.18 × 0.16 × 0.08
no. of rflns collected	86 228	37 760	17 596	17 682
no. of indep rflns (R_{int})	8857 (0.2164)	4361 (0.0817)	5428 (0.1869)	5038 (0.2054)
data/restraints/params	8857/0/523	4361/0/262	5428/6/280	5038/12/267
GOF on F^2	0.846	1.116	1.458	1.042
R1, wR2 ($I > 2\sigma(I)$)	0.0725, 0.1358	0.0595, 0.1204	0.1795, 0.4494	0.1158, 0.2523
R1, wR2 (all data)	0.1971, 0.1792	0.0805, 0.1285	0.2526, 0.4830	0.2047, 0.3059
largest diff peak and hole (e Å^{-3})	0.331, −0.164	0.372, −0.431	3.169, −0.833	1.053, −0.648

LiN_2O_2 coordination mode similar to that of **2** ([(C_5Me_4H)-$B(^{3-Me}pz)_3Li(THF)_2$] and [$(C_5Me_4)B(^{3-Me}pz)_3Li_2(THF)_3$]).[56] Interestingly, the Li−N bond lengths (1.952(8)−1.985(8) Å) of **2** are smaller than those in the other two compounds (2.017(6)−2.039(10) Å), but are similar to the values observed in [$PhB(^{3-tBu}pz)_3Li$][57] (1.934(3), 1.977(3), and 1.979(3) Å), which features an uncommon trigonal Li^+ coordination environment. As already deduced from the ^{11}B NMR spectra, the two boron atoms of **2** are tetracoordinated. Only the C−B−C angles differ significantly from the ideal value (C(1)−B(1)−C(51) = 119.4(3)°; C(2)−B(2)−C(54) = 117.4(3)°). The two *tert*-butyl groups are placed at the same side of the phenylene ring with torsion angles C(1)−B(1)−C(51)−C(56) and C(2)−B(2)−C(54)−C(53) of −24.7(6) and −25.0(6)°, respectively. With respect to the B(1)···B(2) axis, the two *t*BuBpz$_2$ fragments are oriented in an anticlinal conformation (C(1)−B(1)···B(2)−C(2) = 144.6(3)°).

The manganese complex **3a** crystallizes in the form of colorless blocks from THF/hexane (orthorhombic space group *Pnma*) with 1 equiv of THF in the crystal lattice. Because a crystal structure analysis revealed the solvate molecules to be severely disordered, **3a** was recrystallized from a mixture of tetrahydropyrane (THP) and hexane to give colorless blocks of **3b** (Figure 4). Again, the crystal contains solvent molecules; however, this time they do not suffer from major disorder. Apart from their different ether ligands, **3a** and **3b** establish essentially the same structure. Thus, only **3b** is discussed in this paper, although crystal data and structure details of **3a** and a superposition of both structures are available in the Supporting Information. The complex **3b** crystallizes together with 1 equiv of noncoordinated THP (monoclinic space group *P*2/*c*). The compound forms discrete dinuclear molecules [L[Mn(THP)]$_2$(μ-Cl)$_2$] with crystallographic C_2 symmetry (axis perpendicular to the central phenylene ring) in the solid state. Each manganese atom is coordinated in a square-pyramidal fashion with the parameter τ, calculated according to Reedijk et al.,[58] possessing the almost ideal value of 0.03 ($\tau = 0$: square-pyramidal; $\tau = 1$: trigonal-bipyramidal). The apical position of the pyramid is occupied by THP (Mn(1)−O(41) = 2.191(3) Å), whereas the basal plane is spanned by two pyrazolyl nitrogen atoms and two chloride ions in a cis configuration (distance between the Mn(1) center and the least-squares plane through N(12)/N(22)/Cl(1)/Cl(1)# = 0.181 Å). The Mn−N bond lengths (2.185(3), 2.189(3) Å) are in the typical range for Cl-containing Mn^{II} scorpionates (2.13−2.24 Å).[59−61] All the Mn−Cl bonds within the diamond Mn_2Cl_2 core (Mn(1)−Cl(1) = 2.526(1) Å, Mn(1)−Cl(1)# = 2.528(1) Å) are longer than those usually observed in Mn^{II} scorpionates with terminal chloro ligands (2.27−2.37 Å),[59−61] but lie within the typical range for bridged Mn^{II} chlorides (2.31 −2.60 Å;[62−65] the spin state of the reference compounds has not in all cases been published). The intramolecular Mn···Mn distance of 3.527(1) Å in **3b** is out of the range of a Mn−

(56) Roitershtein, D.; Domingos, Â.; Marques, N. *Organometallics* **2004**, *23*, 3483−3487.
(57) Kisko, J. L.; Hascall, T.; Kimblin, C.; Parkin, G. *J. Chem. Soc., Dalton Trans.* **1999**, 1929−1935.
(58) Addison, A. W.; Rao, T. N.; Reedijk, J.; van Rijn, J.; Verschoor, G. C. *J. Chem. Soc., Dalton Trans.* **1984**, 1349−1356.
(59) Di Vaira, M.; Mani, F. *J. Chem. Soc., Dalton Trans.* **1990**, 191−194.
(60) Brunker, T. J.; Hascall, T.; Cowley, A. R.; Rees, L. H.; O'Hare, D. *Inorg. Chem.* **2001**, *40*, 3170−3176.
(61) Nabika, M.; Seki, Y.; Miyatake, T.; Ishikawa, Y.; Okamoto, K.; Fujisawa, K. *Organometallics* **2004**, *23*, 4335−4337.
(62) Garoufis, A.; Kasselouri, S.; Boyatzis, S.; Raptopoulou, C. P. *Polyhedron* **1999**, *18*, 1615−1620.
(63) Chai, J.; Zhu, H.; Roesky, H. W.; He, C.; Schmidt, H.-G.; Noltemeyer, M. *Organometallics* **2004**, *23*, 3284−3289.
(64) van Albada, G. A.; Mohamadou, A.; Driessen, W. L.; de Gelder, R.; Tanase, S.; Reedijk, J. *Polyhedron* **2004**, *23*, 2387−2391.
(65) Wu, J.-Z.; Bouwman, E.; Mills, A. M.; Spek, A. L.; Reedijk, J. *Inorg. Chim. Acta* **2004**, *357*, 2694−2702.

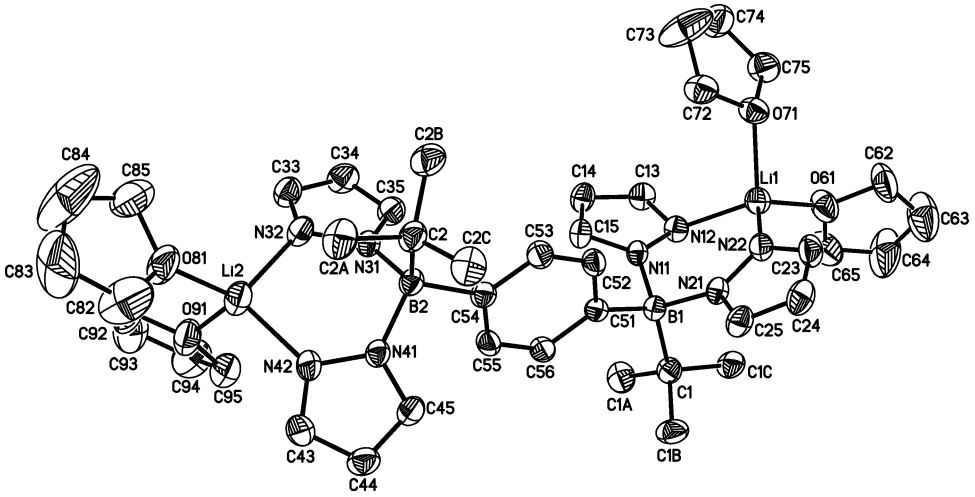

Figure 3. Structure of **2** in the crystal; H atoms omitted for clarity; thermal ellipsoids shown at the 50% probability level. Selected bond lengths (Å), atom···atom distances (Å), bond angles (deg), and torsion angles (deg): Li(1)−N(12) = 1.985(8), Li(1)−N(22) = 1.952(8), Li(2)−N(32) = 1.962(9), Li(2)−N(42) = 1.985(8), B(1)−N(11) = 1.593(5), B(1)−N(21) = 1.586(6), B(1)−C(1) = 1.662(6), B(1)−C(51) = 1.635(6), B(2)−N(31) = 1.597(6), B(2)−N(41) = 1.572(6), B(2)−C(2) = 1.676(6), B(2)−C(54) = 1.641(5); Li(1)···Li(2) = 11.866(10); N(12)−Li(1)−N(22) = 97.5(3), N(32)−Li(2)−N(42) = 97.6(3), N(11)−B(1)−N(21) = 109.5(3), N(31)−B(2)−N(41) = 109.1(3); B(1)−N(11)−N(12)−Li(1) = −52.3(4), B(1)−N(21)−N(22)−Li(1) = −2.8(5), C(1)−B(1)−C(51)−C(56) = −24.7(6), C(2)−B(2)−C(54)−C(53) = −25.0(6), B(2)−N(31)−N(32)−Li(2) = −37.3(5), B(2)−N(41)−N(42)−Li(2) = 8.2(6), C(1)−B(1)···B(2)−C(2) = 144.6(3).

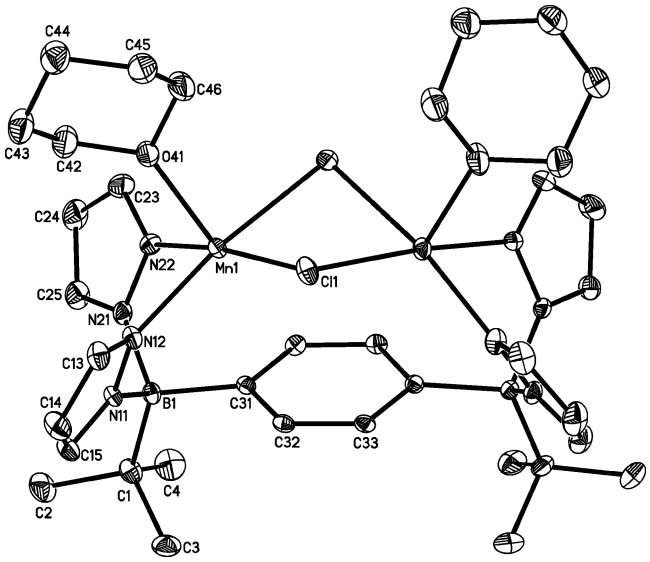

Figure 4. Structure of **3b**·THP in the crystal; H atoms omitted for clarity; thermal ellipsoids shown at the 50% probability level. Selected bond lengths (Å), atom···atom distances (Å), bond angles (deg), and torsion angles (deg): Mn(1)−N(12) = 2.189(3), Mn(1)−N(22) = 2.185(3), Mn(1)−O(41) = 2.191(3), Mn(1)−Cl(1) = 2.526(1), Mn(1)−Cl(1)# = 2.528(1); Mn(1)···C(31) = 2.841(3) Mn(1)···Mn(1)# = 3.527(1); N(12)−Mn(1)−N(22) = 84.3(1), N(12)−Mn(1)−O(41) = 92.6(1), N(12)−Mn(1)−Cl(1) = 95.1(1), N(12)−Mn(1)−Cl(1)# = 172.0(1), N(22)−Mn(1)−O(41) = 92.4(1), N(22)−Mn(1)−Cl(1) = 170.3(1), N(22)−Mn(1)−Cl(1)# = 96.1(1), O(41)−Mn(1)−Cl(1) = 97.3(1), O(41)−Mn(1)−Cl(1)# = 95.4(1), Cl(1)−Mn(1)−Cl(1)# = 83.1(1), Mn(1)−Cl(1)−Mn(1)# = 88.5(1), B(1)···COG(C_6H_4)···B(1)# = 174.4; B(1)−N(11)−N(12)−Mn(1) = −2.5(4), B(1)−N(21)−N(22)−Mn(1) = −9.4(4), C(1)−B(1)−C(31)−C(32) = −87.2(4), N(12)−Mn(1)···Mn(1)#−N(12)# = 120.6(1), N(22)−Mn(1)···Mn(1)#−N(22)# = −115.1(1), O(41)−Mn(1)···Mn(1)#−O(41)# = 3.5(2). Symmetry transformations used to generate equivalent atoms: # $-x+1$, y, $-z+3/2$.

Mn bond (range of Mn−Mn single bond lengths according to a CSD search regarding 510 fragments = 2.391−3.244 Å)[55] and between the values for tetracoordinate (3.275 Å)[63] and hexacoordinate (3.74−3.85 Å)[62,64,65] dinuclear manganese compounds with chloro and nitrogen ligands. In contrast to **2**, the *tert*-butyl groups of **3b** are oriented perpendicular to the C_6H_4 bridge (C(1)−B(1)−C(31)−C(32) = −87.2(4)°). Because the phenylene ring efficiently shields both Mn^{II} centers from coordination of a sixth ligand, the question arises as to what extent the aromatic linker itself might act as donor of π-electron density toward the manganese atoms. In this context, it is noteworthy that the Mn(1)···C(31) distance of 2.841(3) Å is not too much longer than the sum of the half-thickness of benzene (1.7 Å)[66] and the ionic radius of Mn^{II} in its high-spin state (0.89 Å).[67] Moreover, the B−C_6H_4−B backbone is significantly bent (B(1)···COG(C_6H_4)···B(1)# = 174.4°) such that the phenylene ring more closely approaches the Mn_2Cl_2 subunit.

Complexes of **4** (monoclinic, $P2_1/c$) crystallize from methylene chloride at −30 °C in a centrosymmetric conformation as dark red blocks (Figure 5). The crystal lattice contains 2 equiv of solvate molecules. Compound **4** is a rare example of a structurally characterized titanium dimethylamido scorpionate, as only one more record exists in the Cambridge Structural Database,[55] i.e., [(κ^3−HBpz$_3$)Ti(NMe$_2$)$_3$].[68] The two titanium atoms of **4** are separated by 13.187(4) Å, each of them being pentacoordinated by a chelating bis(pyrazol-1-yl)borate unit and three dimethylamido ligands arranged in a propeller-like fashion. With a τ value[58] of 0.48, the coordination polyhedron around each Ti^{IV} center is intermediate between square-pyramidal and trigonal-bipyramidal. The *tert*-butyl groups of **4** are oriented in an antiperiplanar fashion, and the B(1)−C(1) vector is closely aligned with the plane of the central phenylene ring (C(1)−B(1)−C(31)−C(32) = 169.4(10)°). The Ti−N(pz) bonds (2.203(10), 2.229(9) Å) are shorter than those reported

(66) Gokel, G. W.; De Wall, S. L.; Meadows, E. S. *Eur. J. Org. Chem.* **2000**, 2967−2978.
(67) Hollemann, A. F.; Wiberg, N. *Lehrbuch der Anorganischen Chemie*; de Gruyter: Berlin, 1995.
(68) Cai, H.; Lam, W. H.; Yu, X.; Liu, X.; Wu, Z.-Z.; Chen, T.; Lin, Z.; Chen, X.-T.; You, X.-Z.; Xue, Z. *Inorg. Chem.* **2003**, *42*, 3008−3015.

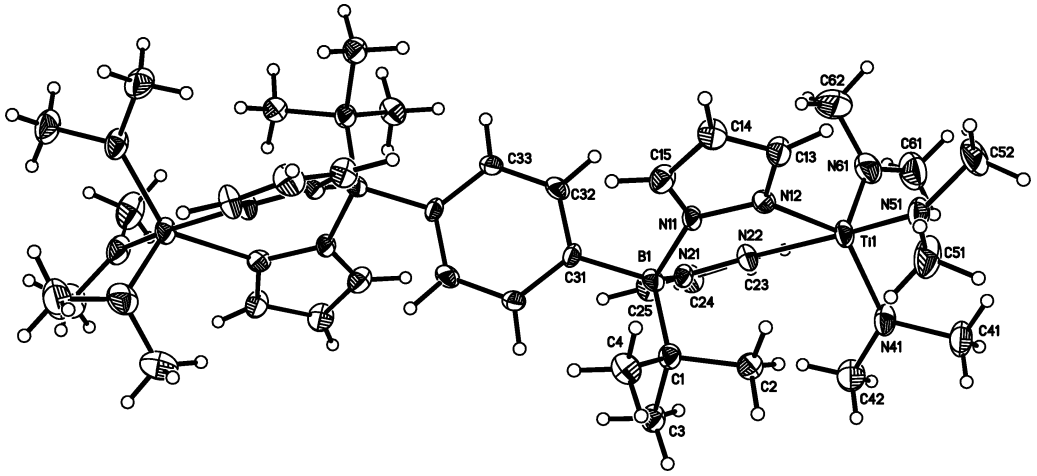

Figure 5. Structure of **4**·$2CH_2Cl_2$ in the crystal; thermal ellipsoids shown at the 50% probability level. Selected bond lengths (Å), atom···atom distances (Å), bond angles (deg), and torsion angles (deg): Ti(1)−N(12) = 2.203(10), Ti(1)−N(22) = 2.229(9), Ti(1)−N(41) = 1.962(10), Ti(1)−N(51) = 1.926(10), Ti(1)−N(61) = 1.882(13); Ti(1)···Ti(1)# = 13.187(4); N(12)−Ti(1)−N(22) = 78.8(3), N(12)−Ti(1)−N(41) = 137.1(4), N(12)−Ti(1)−N(51) = 88.1(4), N(12)−Ti(1)−N(61) = 116.2(5), N(22)−Ti(1)−N(41) = 90.1(4), N(22)−Ti(1)−N(51) = 166.0(4), N(22)−Ti(1)−N(61) = 91.7(4), N(41)−Ti(1)−N(51) = 96.3(4), N(41)−Ti(1)−N(61) = 105.4(5), N(51)−Ti(1)−N(61) = 98.5(5); B(1)−N(11)−N(12)−Ti(1) = 11.4(15), B(1)−N(21)−N(22)−Ti(1) = 6.1(15), C(1)−B(1)−C(31)−C(32) = 169.4(10). Symmetry transformations used to generate equivalent atoms: # $-x + 1$, $-y + 1$, $-z + 1$.

for hexacoordinate [(η^3-HBpz$_3$)Ti(NMe$_2$)$_3$] (2.266(2)−2.298(2) Å),[68] but are equal in length to the Ti−N(pz) bonds in the Ti^{II} complex [(η^3−HBpz$_3$)$_2$Ti] (2.216(2) Å).[69] Compared to the pyrazolyl ligands, the dimethylamido groups of **4** are located at a significantly shorter distance from the titanium centers (1.882(13)−1.962(10) Å) which reflects stronger σ-bonding together with additional p−d π-donation in the latter case (sum of angles around *N*Me$_2$: 360.0(1)°).

Compound **5** crystallizes from toluene/hexane at −20 °C together with one molecule of toluene and one molecule of hexane per formula unit (orange plates; monoclinic, *C*2/*c*). The molecular structure determined by X-ray crystallography is in full agreement with the NMR data of **5**. As in the case of **3b**, **5** consists of discrete dinuclear molecules with crystallographically imposed C_2 symmetry (Figure 6). The 2-fold axis runs through the oxygen atom and the center of gravity of the phenylene ring. Both titanium atoms are connected via an almost linear μ-oxo bridge (Ti(1)−O(1)−Ti(1)# = 175.1(5)°), with Ti−O bond lengths of 1.812(1) Å and an intramolecular Ti···Ti distance of 3.621(3) Å. The only other structurally characterized example of an oxo-bridged titanium poly(pyrazolyl)borate, [[(κ^2-Tp)(κ^3-Tp)Ti^{III}]$_2$(μ-O)] (Tp = [HBpz$_3$]$^-$),[69] features a ligand-unsupported oxygen linker (Ti−O = 1.811(3) Å, Ti−O−Ti = 167.4(1)°) and titanium atoms in their paramagnetic trivalent oxidation state. The titanium atoms of **5** possess distorted square-pyramidal coordination spheres (τ = 0.37)[58] with planar dimethylamido groups occupying the apical positions at a Ti(1)−N(1) distance of 1.878(7) Å. Each bis(pyrazol-1-yl)borate ligand occupies two Ti^{IV} coordination sites with Ti−N bond lengths of 2.187(7) and 2.199(6) Å. These values are only slightly smaller than those in **4** and in [(κ^3-HBpz$_3$)Ti(NMe$_2$)$_3$],[68] and also lie within the range observed for [[(κ^2-Tp)(κ^3-Tp)Ti^{III}]$_2$(μ-O)][69] (2.171(3) and 2.257(3) Å). Compared to **3b**, the phenylene ring in **5** is bent to a lesser extent toward the metal centers (B(1)···COG(C$_6$H$_4$)···B(1)# = 178.3°, Ti(1)···C(31) = 3.067(7) Å).

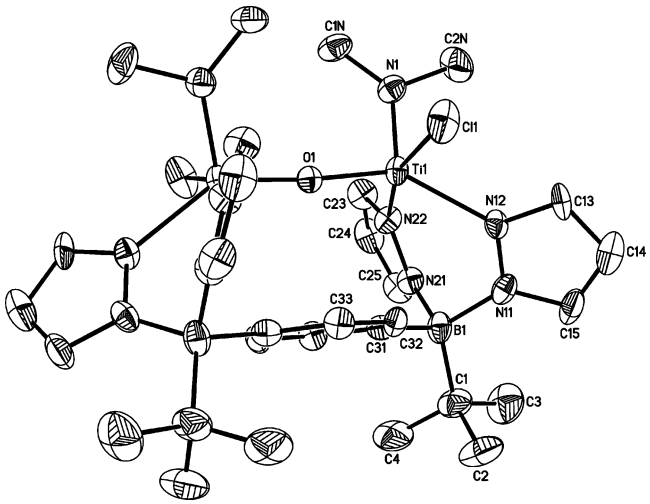

Figure 6. Structure of **5**·C_7H_8·C_6H_{14} in the crystal; H atoms omitted for clarity; thermal ellipsoids shown at the 50% probability level. Selected bond lengths (Å), atom···atom distances (Å), bond angles (deg), and torsion angles (deg): Ti(1)−N(1) = 1.878(7), Ti(1)−N(12) = 2.199(6), Ti(1)−N(22) = 2.187(7), Ti(1)−O(1) = 1.812(1), Ti(1)−Cl(1) = 2.375(2); Ti(1)···C(31) = 3.067(7), Ti(1)···Ti(1)# = 3.621(3); N(1)−Ti(1)−N(12) = 116.3(3), N(1)−Ti(1)−N(22) = 87.7(3), N(12)−Ti(1)−N(22) = 79.9(2), N(1)−Ti(1)−O(1) = 102.1(3), N(12)−Ti(1)−O(1) = 141.6(3), N(22)−Ti(1)−O(1) = 102.2(2), N(1)−Ti(1)−Cl(1) = 96.4(2), N(12)−Ti(1)−Cl(1) = 84.2(2), N(22)−Ti(1)−Cl(1) = 163.7(2), O(1)−Ti(1)−Cl(1) = 92.5(1), Ti(1)−O(1)−Ti(1)# = 175.1(5), B(1)···COG(C$_6$H$_4$)···B(1)# = 178.3; C(1)−B(1)−C(31)−C(32) = 101.3(9), B(1)−N(11)−N(12)−Ti(1) = −0.6(9), B(1)−N(21)−N(22)−Ti(1) = 7.1(9), N(1)−Ti(1)···Ti(1)#−N(1)# = −37.1(3), N(12)−Ti(1)···Ti(1)#−N(12)# = −37.9(4), N(22)−Ti(1)···Ti(1)#−N(22)# = 143.2(2), Cl(1)−Ti(1)···Ti(1)#−Cl(1)# = 156.5(1). Symmetry transformations used to generate equivalent atoms: # $-x + 1$, y, $-z + 3/2$.

Conclusion

Two dinuclear transition-metal compounds, one possessing a bent Mn^{II}−(μ-Cl)$_2$−Mn^{II} core (**3b**) and the other featuring a linear Ti^{IV}−(μ-O)−Ti^{IV} fragment (**5**), have been synthesized using the ditopic bis(pyrazol-1-yl)borate ligand [*p*-C$_6$H$_4$(Bpz$_2$*t*Bu)$_2$]$^{2-}$ (L^{2-}, pz = pyrazol-1-yl). As a result of the

(69) Kayal, A.; Kuncheria, J.; Lee, S. C. *Chem. Commun.* **2001**, 2482−2483.

bridging coordination mode of L^{2-}, both complexes establish macrocyclic structures in which the metal ions are pentacoordinated with square-pyramidal ligand spheres (**3b**: [L[Mn(THP)]$_2$(μ-Cl)$_2$]; **5**: [L[Ti(NMe$_2$)Cl]$_2$(μ-O)]). The intramolecular metal−metal distances in both complexes **3b** and **5** are essentially the same (Mn(1)···Mn(1)# = 3.527(1) Å, Ti(1)···Ti(1)# = 3.621(3) Å), and most likely predetermined by the rigid framework of L^{2-}. Thus, pronounced differences in the ionic radii of the metal centers M^{x+} (r(h.s. Mn^{II}) = 0.89 Å, r(Ti^{IV}) = 0.65 Å)[67] as well as of the bridging elements E^{y-} (r(Cl^-) = 1.67 Å, r(O^{2-}) = 1.21 Å)[67] are counterbalanced by the bent, diamond core M−(μ-E)$_2$−M in the case of the larger ions as opposed to the almost-linear M−(μ-E)−M arrangement adopted by the smaller ions constituting the Ti−O−Ti bridge. As all bonds established by the metal centers M^{x+} are very similar in length to those of related reference molecules, it is immediately apparent that both M−(μ-E)$_z$−M (z = 1, 2) core units are perfectly adjusted to the geometric requirements of the ditopic ligand L^{2-}.

In **3b** and **5**, the scorpionate ligand efficiently shields half of the coordination sphere of each metal atom. On the other hand, it provides only two σ-donor sites for ion complexation. A third coordination site of each metal is forced to remain vacant for steric reasons. However, the phenylene ring may in part be able to compensate for that by providing π-electron density from its phenylene spacer. It is interesting to note in this context that the B−C$_6$H$_4$−B fragment of **3b** is slightly bent such that the phenylene ring is pushed toward the manganese ions (Mn(1)···C(31) = 2.841(3) Å, B(1)···COG(C$_6$H$_4$)···B(1)# = 174.4°; B(1) is located 0.151 Å below the best plane through the phenylene ring). Similarly close metal−arene contacts were also observed in Tl^I and Ag^I complexes of the ditopic scorpionate [m-C$_6$H$_4$(Bpz$_2$$t$Bu)$_2$]$^{2-}$ **D** which is closely related to L^{2-}.[18] The finding that B−C$_6$H$_4$−B bending is less pronounced in the titanium complex **5** may either be due to the fact that Ti^{IV} is commonly pentacoordinated or due to the presence of the strongly π-donating NMe$_2$ group trans to the phenylene ring.

The examples of **3** and **5** clearly demonstrate that the ditopic scorpionate ligand [p-C$_6$H$_4$(Bpz$_2$$t$Bu)$_2$]$^{2-}$ is well-designed to bring two metal centers into such proximity that they can act simultaneously on the same substrate molecule. This is an essential quality for gaining benefits from cooperative effects between the two metal centers with respect to possible applications in homogeneous catalysis.

The shape of the ligand pocket and the pyrazolyl functionalities of L^{2-} is reminiscent of protein cavities in metal-containing enzymes featuring imidazolyl side chains of histidine (e.g., methane monooxygenase,[70] arginase,[22] and catalase[22]). In the future, we will therefore explore the potential of L^{2-} for the design of bioinorganic model systems.

Experimental Section

General Considerations. All reactions and manipulations of air-sensitive compounds were carried out in dry, oxygen-free nitrogen or argon using standard Schlenk ware. Solvents were freshly distilled under argon from Na−benzophenone (toluene, THF, THP) or Na/Pb alloy (hexane), or were stored over 4 Å molecular sieves prior to use (C_6D_6, CH_2Cl_2). NMR: Bruker AMX 400, Bruker AMX 250, Bruker DPX 250 spectrometers. ^{11}B NMR spectra are reported relative to external BF_3·Et_2O. Unless stated otherwise, all NMR spectra were run at ambient temperature. Abbreviations: s = singlet, d = doublet, vtr = virtual triplet, dd = doublet of doublets, br = broad, n.o. = signal not observed; Me = methyl, Ph = phenyl, pz = pyrazol-1-yl, THF = tetrahydrofuran, THP = tetrahydropyran, COG = center of gravity. p-C$_6$H$_4$[B(NMe$_2$)tBu]$_2$ **1**,[14] [Ti(NMe$_2$)$_3$Cl], and [Ti(NMe$_2$)$_2$Cl$_2$][53] were synthesized according to literature procedures. Pyrazole was purchased from Aldrich.

Synthesis of LLi$_2$(THF)$_4$, 2. To a stirred solution of p-C$_6$H$_4$[B(NMe$_2$)tBu]$_2$ (**1**) (7.209 g, 24.02 mmol) in toluene (40 mL) and THF (20 mL) were added at ambient temperature neat lithium pyrazolide (3.555 g, 48.04 mmol) and neat pyrazole (3.271 g, 48.04 mmol). After the resulting solution had been heated to reflux temperature for 8 h, the solvent was evaporated; the white solid residue was washed with toluene (2 × 5 mL) and hexane (5 mL), and dried in vacuo. Yield: 16.694 g (21.33 mmol, 89%). Crystals suitable for an X-ray crystal structure analysis were grown by layering a concentrated THF solution of **2** with toluene (1:3). ^{11}B NMR (128.4 MHz, d$_8$-THF): δ 3.0 ($h_{1/2}$ = 390 Hz). ^{1}H NMR (400.1 MHz, d$_8$-THF): δ 0.66 (s, 18H, CCH$_3$), 5.93 (vtr, 4H, $^3J_{HH}$ = 2.0 Hz, pzH-4), 7.05 (dd, 4H, $^3J_{HH}$ = 2.2 Hz, $^4J_{HH}$ = 0.7 Hz, pzH-3 or -5), 7.33 (s, 4H, C$_6$H$_4$), 7.42 (dd, 4H, $^3J_{HH}$ = 1.7 Hz, $^4J_{HH}$ = 0.7 Hz, pzH-5 or -3). ^{13}C NMR (62.9 MHz, d$_8$-THF): δ 30.5 (C*C*H$_3$), 102.1 (pzC-4), 135.0 (C$_6$H$_4$), 137.7, 137.9 (pzC-3,5), n.o. (CB).

Synthesis of [L[Mn(THF)]$_2$(μ-Cl)$_2$], 3a. A solution of [LLi$_2$(THF)$_4$] (**2**; 1.399 g, 1.79 mmol) in THF (20 mL) was added with stirring at ambient temperature to a suspension of MnCl$_2$ (0.450 g, 3.58 mmol) in THF (20 mL). After 10 min, the reaction mixture turned into a pale yellow solution, and was stirred for 10 h. The solvent was evaporated, and the white residue recrystallized from THF/hexane (1:3) to give colorless crystals of **3a**·THF. Yield: 0.900 g (1.12 mmol, 62%). Recrystallization of **3a** from THP/hexane gave X-ray quality crystals of **3b**·THP ([L[Mn(THP)]$_2$(μ-Cl)$_2$]·THP). Anal. Calcd for $C_{38}H_{58}B_2Cl_2Mn_2N_8O_3$ (877.32): C, 52.02; H, 6.66; N, 12.77. Found: C, 51.70; H, 6.54; N, 12.43.

Synthesis of [L[Ti(NMe$_2$)$_3$]$_2$], 4. A solution of [LLi$_2$(THF)$_4$] (**2**; 0.508 g, 0.65 mmol) in toluene (10 mL) was cooled to −78 °C and added via cannula to a chilled solution of [Ti(NMe$_2$)$_3$Cl] (0.280 g, 1.30 mmol) in toluene (10 mL). After 30 min, the reaction mixture was warmed to room temperature and stirred for 8 h. All volatiles were removed in vacuo. The crude product **4** was then separated from LiCl by extraction into hexane (2 × 5 mL). After evaporation of the extract, the red residue was dissolved in methylene chloride and stored at −30 °C to give dark red crystals of **4**·2CH$_2$Cl$_2$ suitable for X-ray crystallography. Yield of **4**: 0.333 g (0.40 mmol, 62%). ^{11}B NMR (128.4 MHz, C$_6$D$_6$): δ 3.7 ($h_{1/2}$ = 390 Hz). ^{1}H NMR (250.1 MHz, C$_6$D$_6$): δ 1.25 (br, 18H, CCH$_3$), 3.06 (s, 36H, NCH$_3$), 6.02 (vtr, 4H, $^3J_{HH}$ = 2.2 Hz, pzH-4), 7.31 (s, 4H, C$_6$H$_4$), 7.39, 7.63 (2 × d, 2 × 4H, $^3J_{HH}$ = 2.2 Hz, pzH-3,5). ^{13}C NMR (62.9 MHz, C$_6$D$_6$): δ 30.5 (C*C*H$_3$), 47.8 (NCH$_3$), 104.0 (pzC-4), 133.9 (C$_6$H$_4$), 138.9, 142.4 (pzC-3,5), n.o. (CB).

Synthesis of [L[Ti(NMe$_2$)Cl]$_2$(μ-O)], 5. To a chilled solution of [Ti(NMe$_2$)$_2$Cl$_2$] (0.166 g, 0.80 mmol) in THF (20 mL) was added H$_2$O (0.007 g, 0.40 mmol; calibrated solution in THF) with stirring. After 10 min, a solution of [LLi$_2$(THF)$_4$] (**2**; 0.314 g, 0.40 mmol) in THF (10 mL) was added via cannula at −78 °C. After being stirred for 1 h, the reaction mixture was warmed to room

(70) Que, L., Jr.; Tolman, W. B. *Angew. Chem., Int. Ed.* **2002**, *41*, 1114−1137.

temperature and stirred for another 10 h. The solvent was removed in vacuo, and the residue was washed with hexane (10 mL), dissolved in a 1:1 mixture of toluene and hexane, and cooled to −20 °C to give orange X-ray quality crystals of **5**·C_7H_8·C_6H_{14}. Yield of **5**·C_7H_8·C_6H_{14}: 0.233 g (0.25 mmol, 63%). ^{11}B NMR (128.4 MHz, d_8-THF): δ 0.9 ($h_{1/2}$ = 330 Hz). ^{11}B NMR (128.4 MHz, C_6D_6): δ 2.9 ($h_{1/2}$ = 380 Hz). ^{1}H NMR (400.1 MHz, d_8-THF): δ 1.15 (br, 18H, CCH_3), 3.67 (s, 12H, NCH_3), 6.25 (vtr, 2H, $^3J_{HH}$ = 2.3 Hz, pzH-4), 6.28 (dd, 2H, $^3J_{HH}$ = 7.5 Hz, $^4J_{HH}$ = 1.7 Hz, C_6H_4), 6.32 (vtr, 2H, $^3J_{HH}$ = 2.3 Hz, pzH-4′), 6.55 (dd, 2H, $^3J_{HH}$ = 7.5 Hz, $^4J_{HH}$ = 1.7 Hz, C_6H_4), 7.53 (dd, 2H, $^3J_{HH}$ = 2.3 Hz, $^4J_{HH}$ = 0.5 Hz, pzH-3 or -5), 8.13 (dd, 2H, $^3J_{HH}$ = 2.3 Hz, $^4J_{HH}$ = 0.5 Hz, pzH-5 or -3), 8.16 (dd, 2H, $^3J_{HH}$ = 2.3 Hz, $^4J_{HH}$ = 0.6 Hz, pzH-3′ or -5′), 8.24 (dd, 2H, $^3J_{HH}$ = 2.3 Hz, $^4J_{HH}$ = 0.6 Hz, pzH-5′ or -3′). ^{1}H NMR (400.1 MHz, C_6D_6): δ 1.19 (br, 18H, CCH_3), 3.36 (s, 12H, NCH_3), 5.95 (vtr, 2H, $^3J_{HH}$ = 2.3 Hz, pzH-4), 6.01 (vtr, 2H, $^3J_{HH}$ = 2.2 Hz, pzH-4′), 6.63, 6.84 (2 × dd, 2 × 2H, $^3J_{HH}$ = 7.5 Hz, $^4J_{HH}$ = 1.6 Hz, C_6H_4), 7.44, 7.85 (2 × d, 2 × 2H, $^3J_{HH}$ = 2.2 Hz, pzH-3′,5′), 7.92, 8.26 (2 × d, 2 × 2H, $^3J_{HH}$ = 2.2 Hz, pzH-3,5). ^{13}C NMR (62.9 MHz, d_8-THF): δ 30.6 (CCH_3), 50.8 (NCH_3), 104.0 (pzC-4′), 104.4 (pzC-4), 130.7 (C_6H_4), 135.5 (pzC-5 or -3), 137.3 (pzC-5′ or -3′), 138.4 (C_6H_4), 142.6 (pzC-3 or -5), 143.8 (pzC-3′ or -5′), n.o. (CB). ^{13}C NMR (62.9 MHz, C_6D_6): δ 29.3 (CCH_3), 50.3 (NCH_3), 102.9 (pzC-4′), 103.4 (pzC-4), 129.3 (C_6H_4), 134.3 (pzC-3′ or -5′), 135.9 (pzC-3 or -5), 137.8 (C_6H_4), 140.8 (pzC-5′ or -3′), 142.3 (pzC-5 or -3), n.o. (CB). Anal. Calcd for $C_{43}H_{68}B_2Cl_2N_{10}OTi_2$ (929.39): C, 55.57; H, 7.37; N, 15.07. Found: C, 55.31; H, 7.32; N, 14.88.

Crystal Structure Determinations of 2, 3a·THF, 3b·THP, 4·2CH_2Cl_2, and 5·C_7H_8·C_6H_{14}. Data collection was performed on a Stoe-IPDS-II two-circle diffractometer with graphite-monochromated Mo Kα radiation. An empirical absorption correction with the MULABS option[71] in the program PLATON[72] was performed. The structure was solved by direct methods,[73] and refined with full-matrix least-squares on F^2 using the program SHELXL97.[74] Hydrogen atoms were placed on ideal positions, and refined with fixed isotropic displacement parameters using a riding model.

The solvent THF in **3a**·THF is located on a crystallographic mirror plane and disordered over two positions. Its atoms were isotropically refined. The tetrahydropyran solvent molecule in **3b**·THP is disordered about a crystallographic 2-fold rotation axis. The crystals of **4** and **5** contain solvate molecules (CH_2Cl_2 in the case of **4**, hexane and toluene in the case of **5**) that are severely disordered. This has a negative effect on the figures of merit of the crystal structures. The anisotropic displacement parameter of the carbon atom of the CH_2Cl_2 molecule in **4**·2CH_2Cl_2 was restrained to an isotropic behavior. The atoms of the hexane solvent in **5**·C_7H_8·C_6H_{14} were refined isotropically.

CCDC reference numbers: 277679 (**2**), 277680 (**3a**·THF), 277681 (**3b**·THP), 277682 (**4**·2CH_2Cl_2), 277683 (**5**·C_7H_8·C_6H_{14}).

Acknowledgment. This research was generously supported by the Deutsche Forschungsgemeinschaft (DFG) and the Fonds der Chemischen Industrie (FCI). The authors are grateful to M.Sc. Katarina Removic-Langer for the SQUID measurements.

Supporting Information Available: Crystallographic data of **2**, **3a**·THF, **3b**·THP, **4**·2CH_2Cl_2, and **5**·C_7H_8·C_6H_{14} in CIF format; superposition of the molecular structures of **3a** and **3b**. This material is available free of charge via the Internet at http://pubs.acs.org.

IC051689H

(71) Blessing, R. H. *Acta Crystallogr., Sect. A* **1995**, *51*, 33−38.
(72) Spek, A. L. *Acta Crystallogr., Sect. A* **1990**, *46*, C34.
(73) Sheldrick, G. M. *Acta Crystallogr., Sect. A* **1990**, *46*, 467−473.
(74) Sheldrick, G. M. *SHELXL-97, A Program for the Refinement of Crystal Structures*; Universität Göttingen: Göttingen, Germany, 1997.